Machining of Metal Matrix Composite Using Abrasive Water Jet Machine

E. Soundrapandian, A. Tajdeen, K. Kamal Basha, and P. Vivekkumar

Abstract Abrasive water jet machining (AWJM) is one of the unconventional machining processes, in which the material is removed by the impact of high-pressure water, along with entrained abrasives. The input parameters involved in the AWJM system are water jet pressure, abrasive flow rate, orifice diameter, nozzle diameter, particle size of the abrasive, abrasive type, etc. Metal matrix composites (MMC) are widely used in the industries such as automobile, defense and aerospace. This work is an attempt to study on machinability of aluminum alloy 7074 (Al 7074) reinforcement with 10% silicon carbide (SiC) particulate. AWJM experiments were conducted on trapezoidal-shaped metal matrix composite by varying abrasive mesh size, abrasive flow rate, water jet pressure and traverse rate to obtain higher material removal rate, depth of cut and better surface finish. The experiments are carried out based on response surface methodology (RSM) designed using Box–Behnken method for four parameters into three levels. Using response surface graph, the significant AWJM machining parameters and their levels are identified to achieve higher material removal rate, depth of cut and better surface finish.

Keywords Abrasive water jet machining · Metal matrix composite · Machinability · Response surface methodology

1 Introduction

In abrasive water jet machining, kerf top width and taper angle were influenced by the parameters such as transverse speed, standoff distance and mass flow rate [1]. The standoff distance has a predominant influence on the workpiece quality, and also the RMS and ACS values are lower when machining lower thickness workpiece [2]. In order to evaluate the Ra on the machined surface of MMC, increased in Ra value was observed due to increase in water jet pressure [3]. In the cases

E. Soundrapandian (✉) · A. Tajdeen · K. K. Basha · P. Vivekkumar
Department of Mechanical Engineering, Bannari Amman Institute of Technology, Sathyamangalam, Erode 638401, Tamil Nadu, India
e-mail: soundrapandian@bitsathy.ac.in

G. Kumaresan et al. (eds.), *Advances in Materials Research*, Springer Proceedings in Materials 5, https://doi.org/10.1007/978-981-15-8319-3_30

of slot cutting and piercing in MMC, the kerf taper will increase with increase in transfer rate and particle size but in the case of piercing kerf taper increases with increase in standoff distance [4]. On varying the abrasive mass flow rate, abrasive mesh size and jet impact angles on MMC found that erosion rate increases with increase in jet impact angles [5]. In machining of MMC, the depth of cut is higher when the mesh size is lesser due to lesser kinetic energy of the smaller size aggregate [6]. The machining aspects of MMCs were carried out in various non-conventional machining processes such as EDM, laser cutting and AWJM; in AWJM the mechanism of material removal was observed as ductile shearing and also there were no thermal damage and burr formation in the AWJM [7]. The process parameters of AWJM greatly influence its machining performance. It is widely classified into four types, namely [8] abrasive parameters: abrasive mass flow rate, abrasive size distribution, abrasive particle shape, diameter and hardness, etc.; [9] cutting parameters: standoff distance, impact angle, number of passes, traverse rate, etc.; mixing chamber and acceleration parameters: focusing nozzle length, focusing nozzle inside diameter, etc., and [10–12] hydraulic parameters: water flow rate, pump pressure, orifice diameter, etc. Each of these parameters has been investigated by several researchers using experimental trials and their optimum values have been found. These values become indispensable when one advances toward condition monitoring [13]. For any process to be completely automated and monitored, an in-depth understanding of the interaction between the machine, workpiece and tool is required. Hence, condition monitoring of AWJM is of primary importance for full automation. Condition monitoring is the continuous/periodic verification of few or all parameters of the system. It is usual to make sure that all system components are performing in close agreement to the optimum level or as a fault detection system [14, 15]. A comprehensive review on major research activity carried out so far by several researchers on condition monitoring of AWJM is also discussed here.

2 Experiment Details

2.1 MMC Casting Procedures

An electric furnace is used for preheating the reinforcements, and electric resistance furnace is used for melting the matrix material. MMCs are made by liquid-state stir casing process. The stir casting furnace is used for preheating the reinforcement of Si at the temperature of 700 °C. The trapezoid-shaped die is used for preparing the workpieces. The size of the workpieces is 10 mm diameter rods. Casted component (Al7074 alloy with 10% of SiC) is a poured in trapezoid-shaped die.

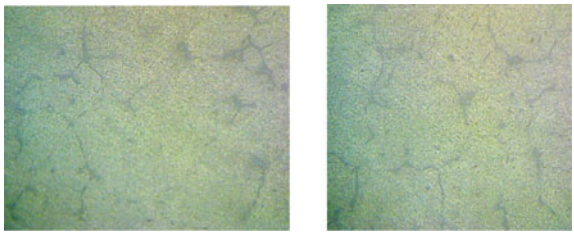

Fig. 1 Optical micrographs of MMCS

a)Al 7074 + 10% SiC **b)Al 7074 + 10% SiC**

2.2 Microstructure

To study the microstructure of the specimens, they were cut and prepared as per the standard metallographic procedure. The specimen plates were prepared by grinding through 600 mesh size grit abrasives. Velvet cloth was polished by using 240, 400, 600 and 1000 mesh size to get the fine surface finish. After that specimens were further polished by using Nital reagent (etched). All these specimens were kept in dry air. The microstructure etched specimens were observed using optical microscope. The presence of SiC in the composites materials has been identified using microscope images captured with (Dewinter Metallurgical Microscope). It is observed from Fig. 1 the uniform distribution of SiC particles. This can be attributed to the effective stirring action and the use of appropriate process parameter.

2.3 Response Surface Methodology (RSM)

In this technique, the main objective is to optimize the response surface that is influenced by various process parameters. RSM also quantifies the relationship between the controllable input parameters and the obtained response surfaces.

If all variables are assumed to be measurable, the response surface can be expressed as follows:

$$Y = f(X_1, X_2, \ldots, X_n)$$

where

Y is the answer of the system and is the variable of action called factors.

The goal is to optimize the response variable y. In this work, the response y is MRR and Ra.

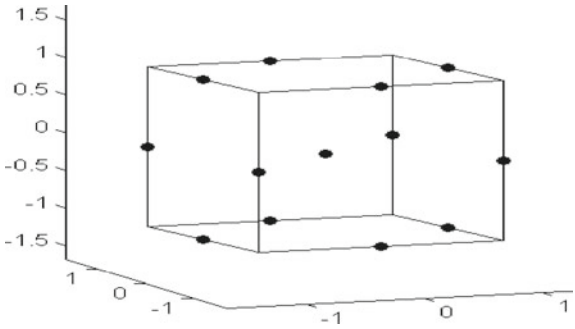

Fig. 2 Box–Behnken design

2.4 Box–Behnken Design

In this study, the Box–Behnken experimental design was chosen for finding out optimized WEDT parameters and regression equations which gives the relationship between the response functions (MRR and Ra) and variables pulse on time, voltage, spindle speed and pulse off time. Box–Behnken design is rotatable second-order designs based on three-level fractional factorial designs. The geometry of a Box–Behnken design is shown in Fig. 2.

Reason for the selection of Box–Behnken design over central composite design is for fewer no. of input factors (here four) and lesser no. of experiments are required than central composite design.

2.5 Level Input Parameter Using RSM

See Tables 1 and 2.

3 Result and Discussion

See Table 3.

Table 1 AWJM input parameters

S. No.	Description	Low	Medium	High
1	Water jet pressure (MPa)	124	200	274
2	Abrasive flow rate (g/min)	240	340	440
3	Abrasive mesh size (#)	80	100	120
4	Traverse speed (mm/min)	60	90	120

Table 2 Observation results

S. No.	Abrasive mesh size (#)	Abrasive flow rate (g/min)	Water jet pressure (Mpa)	Traverse rate (mm/min)	Metal removal rate (mm^3/min)	Depth of cut (mm)	Kerf tapper angle (°)	Surface roughness (μm)
1	80	240	200	90	677	20.04	0.1	4.067
2	120	240	200	90	491	14.44	0.2	3.047
3	80	440	200	90	844	24.03	0.0	3.647
4	120	440	200	90	423	14.4	0.1	2.32
4	100	340	124	60	410	18.24	0.1	2.708
6	100	340	274	60	422	23.18	0.1	3.294
7	100	340	124	120	402	11.14	0.2	3.479
8	100	340	274	120	409	11.3	0.3	3.377
9	80	340	200	60	424	23.27	0.2	3.383
10	120	340	200	60	230	10.2	0.2	3.032
11	80	340	200	120	423	9.4	0.4	2.367
12	120	340	200	120	414	9.21	0.4	2.44
13	100	240	124	90	440	13.33	0.2	3.969
14	100	440	124	90	442	13.39	0.1	2.397
14	100	240	274	90	444	13.14	0.2	3.439
16	100	440	274	90	443	16.1	0.2	3.012
17	80	340	124	90	400	14.82	0.2	3.424
18	120	340	124	90	374	11.1	0.2	3.27
19	80	340	274	90	447	16.2	0.1	3.449
20	120	340	274	90	343	10.14	0.2	2.647
21	100	240	200	60	333	14.8	0.1	3.114
22	100	440	200	60	340	14.1	0.2	3.197
23	100	240	200	120	371	8.24	0.4	2.716
24	100	440	200	120	619	13.76	0.4	3.447
24	100	340	200	90	474	14.06	0.3	4.727
26	100	340	200	90	491	14.44	0.3	2.342
27	100	340	200	90	491	14.44	0.2	2.444
28	100	340	200	90	407	14.03	0.2	3.146
29	100	340	200	90	491	14.44	0.3	3.889

3.1 Response Surface Methodology

See Fig. 3.

Table 3 Box–Benkhen L29 I/O parameter

S. No.	Abrasive mesh size (#)	Abrasive flow rate (g/min)	Water jet pressure (MPa)	Traverse rate (mm/min)	Metal removal rate (mm^3/min) Al + 10% SiC	DoC (mm)	Surface roughness (μm)
1	80–120	240–440	125	60	647.448	22.354	2.21
2	80–120	240–440	200	60	630.845	25.919	2.21
3	80–120	240–440	275	60	615.327	28.701	2.42
4	80–120	240–440	125	90	457.579	19.080	2.51
5	80–120	240–440	200	90	591.829	21.447	2.59
6	80–120	240–440	275	90	626.155	23.032	2.72
7	80–120	240–440	125	120	381.547	13.961	2.68
8	80–120	240–440	200	120	527.505	15.131	2.58
9	80–120	240–440	275	120	590.015	15.518	2.29
10	80–120	240	125–275	60	631.011	25.391	2.84
11	80–120	340	125–275	60	612.223	26.076	2.59
12	80–120	440	125–275	60	624.928	28.701	2.21
13	80–120	240	125–275	90	521.571	17.157	2.75
14	80–120	340	125–275	90	558.8	19.105	2.73
15	80–120	440	125–275	90	627.376	23.032	2.51
16	80–120	240	125–275	120	373.165	11.601	2.21
17	80–120	340	125–275	120	466.296	11.436	2.36
18	80–120	440	125–275	120	590.015	15.518	2.54
19	80–120	240	125	60–120	586.69	21.934	3.30
20	80–120	240	200	60–120	630.845	24.054	2.75
21	80–120	240	275	60–120	534.283	25.391	2.21
22	80–120	340	125	60–120	534.023	21.174	2.59
23	80–120	340	200	60–120	609.134	24.017	2.58
24	80–120	340	275	60–120	584.321	26.076	2.36
25	80–120	440	125	60–120	503.117	22.354	2.21
26	80–120	440	200	60–120	609.575	25.919	2.23
27	80–120	440	275	60–120	627.851	28.701	2.42
28	80	240–440	125–275	60	631.011	28.701	2.55
29	100	240–440	125–275	60	393.444	20.192	2.37
30	120	240–440	125–275	60	192.263	13.482	2.21
31	80	240–440	125–275	90	627.376	22.853	2.98
32	100	240–440	125–275	90	467.009	17.651	2.97
33	120	240–440	125–275	90	343.035	13.507	2.53

(continued)

Table 3 (continued)

S. No.	Abrasive mesh size (#)	Abrasive flow rate (g/min)	Water jet pressure (MPa)	Traverse rate (mm/min)	Metal removal rate (mm^3/min) Al + 10% SiC	DoC (mm)	Surface roughness (μm)
34	80	240–440	125–275	120	590.015	15.518	2.77
35	100	240–440	125–275	120	537.946	13.669	2.67
36	120	240–440	125–275	120	521.431	13.311	3.37
37	80	240–440	125	60–120	586.69	22.354	2.56
38	100	240–440	125	60–120	367.856	16.601	2.41
39	120	240–440	125	60–120	381.547	13.211	2.12
40	80	240–440	200	60–120	630.845	25.919	3.24
41	100	240–440	200	60–120	497.521	18.138	2.81
42	120	240–440	200	60–120	498.8	13.389	2.22
43	80	240–440	275	60–120	627.851	28.701	2.87
44	100	240–440	275	60–120	537.441	20.192	2.67
45	120	240–440	275	60–120	516.13	13.518	2.31
46	80	240	125–275	60–120	631.011	25.391	2.78
47	100	240	125–275	60–120	397.42	18.892	2.71
48	120	240	125–275	60–120	364.411	13.482	2.23
49	80	340	125–275	60–120	612.298	26.076	3.43
50	100	340	125–275	60–120	428.849	18.572	2.92

3.2 Analysis of MRR for Al 7075 + 10% SiC

Table 3 (S. No. 1–9) indicates that MRR values are achieved by varying abrasive mesh size (#80–#120) and abrasive flow rate (240–440 g/min), while water jet pressure and traverse rate are varied at different levels of combinations. Among the combinations, it is observed that high water jet pressure and low traverse rate result in high MRR of 647 mm^3/min. From the analysis (Table 3, S. No. 1–54 and Fig. 4), it is observed that the combinations of input process parameter and their levels such as low abrasive mesh size, high abrasive flow rate, high water jet pressure and low traverse rate result in high MRR(648 mm^3/min) for Al 7075 + 10% SiC. It is observed that higher MRR is achieved with size (#80) and lower MRR is achieved with size (#120). Due to the fact that smaller size of abrasive is likely to possess lesser kinetic energy than resulting in lower MRR, higher size of abrasive is likely to possess higher kinetic energy than resulting in higher MRR.

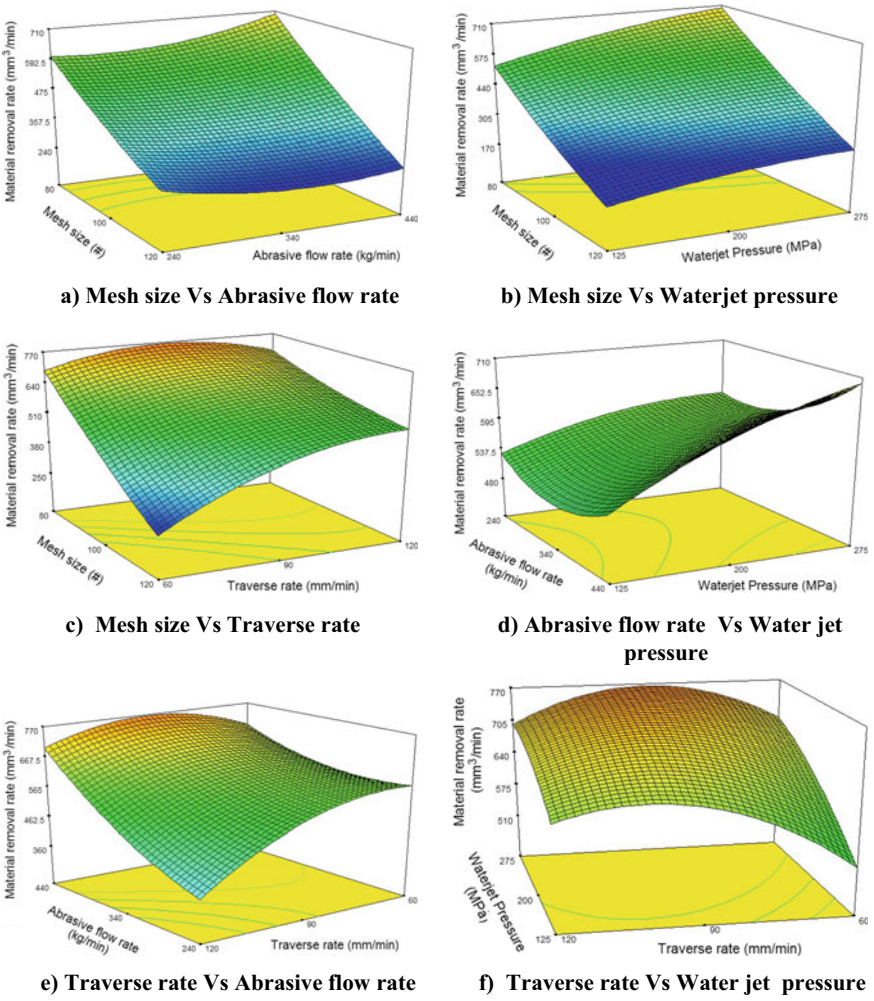

a) Mesh size Vs Abrasive flow rate

b) Mesh size Vs Waterjet pressure

c) Mesh size Vs Traverse rate

d) Abrasive flow rate Vs Water jet pressure

e) Traverse rate Vs Abrasive flow rate

f) Traverse rate Vs Water jet pressure

Fig. 3 Response surface of MRR (Al 7075 + 10% SiC) for various combinations

The relationship between the input process parameter and the response (MRR) for MMC is expressed in the form of regression equation, and it is given below.

$$\begin{aligned}\text{MRR Al 7075} + 10\%\ \text{SiC} = {} & +3977.58 - (28.00 * \text{MS}) - (5.43 * \text{AFR}) \\ & + (4.98 * \text{WP}) - (24.21 * \text{TR}) - (8.14\text{E} - 003 * \text{MS} * \text{AFR}) \\ & - (0.030 * \text{MS} * \text{WP}) + (0.25 * \text{MS} * \text{TR}) + (8.25\text{E} - 004 * \text{AFR} * \text{WP}) \\ & + (0.031 * \text{AFR} * \text{TR}) + (0.025 * \text{WP} * \text{TR}) - (0.015 * \text{MS2}) \\ & + (3.42\text{E} - 003 * \text{AFR2}) - (0.015 * \text{WP2}) - (0.079 * \text{TR2})\end{aligned}$$

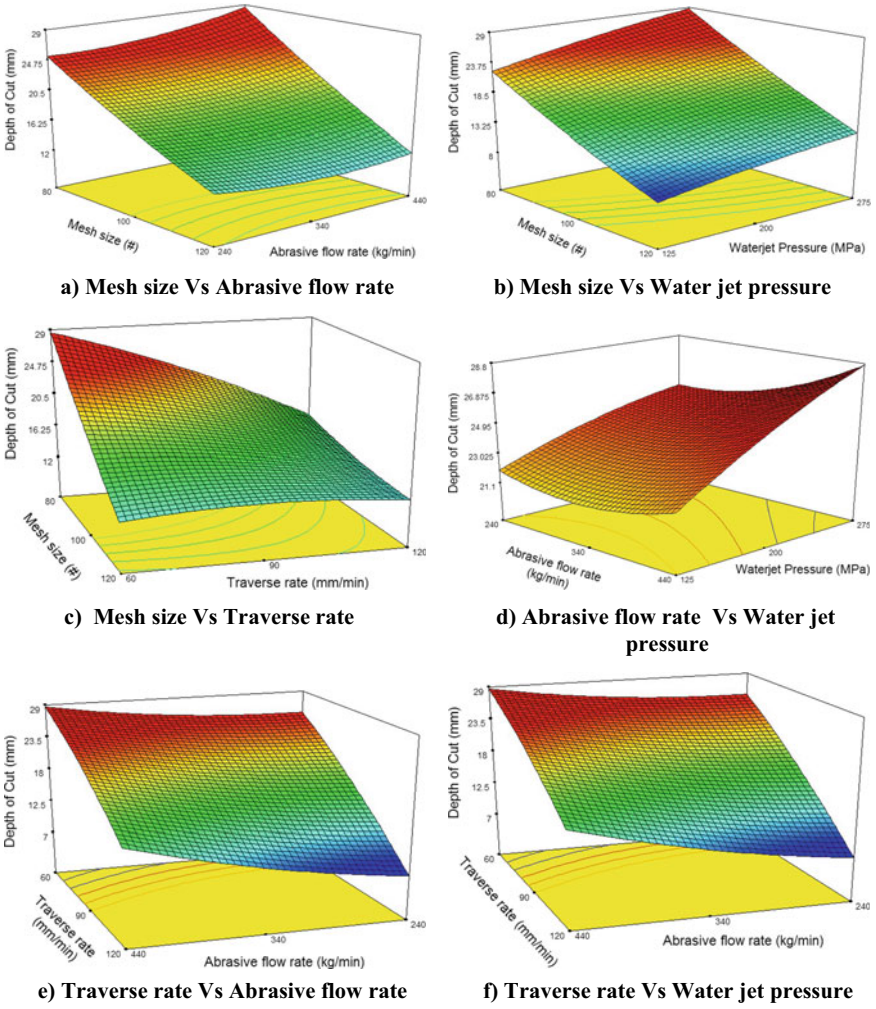

a) Mesh size Vs Abrasive flow rate

b) Mesh size Vs Water jet pressure

c) Mesh size Vs Traverse rate

d) Abrasive flow rate Vs Water jet pressure

e) Traverse rate Vs Abrasive flow rate

f) Traverse rate Vs Water jet pressure

Fig. 4 Response surface of DoC (Al 7075 + 10% SiC) for various combinations

3.3 Analysis of DoC for Al 7075 + 10%SiC

Table 5 (S. No. 1–9) indicates that DOC values are achieved by varying abrasive mesh size (#80–#120) and abrasive flow rate (240–440 g/min), while water jet pressure and traverse rate are varied at different levels of combinations. Among the combinations, it is observed that high water jet pressure and low traverse rate result in high DOC of 29 mm (Table 3 S. No. 3). Due to the fact that smaller size of abrasive is likely to possess lesser kinetic energy than resulting in lower DOC, higher size of abrasive is likely to possess higher kinetic energy than resulting in higher DOC. Similarly,

Table 4 Analysis of variance table for MRR (Al 7075 + SiC 10%)

Source	Sum of squares	d*f*	Mean square	*F* value	*p*-value prob > *F*	
Model	368.628	14	26.3302	3.209775	0.0184	Significant
A-abrasive-e mesh	120.7771	1	120.7771	14.72329	0.0018	
B-AFR	18.1548	1	18.1548	2.213155	0.1590	
C-water pressure	5.400208	1	5.400208	0.658311	0.4307	
D-reverse rate	145.0465	1	145.0465	17.68185	0.0009	
AB	4.0401	1	4.0401	0.492507	0.4943	
AC	1.357225	1	1.357225	0.165452	0.6903	
AD	41.4736	1	41.4736	5.055826	0.0412	
BC	2.088025	1	2.088025	0.25454	0.6217	
BD	6.786025	1	6.786025	0.827248	0.3785	
CD	5.736025	1	5.736025	0.699248	0.4171	
A^2	1.812327	1	1.812327	0.220931	0.6456	
B^2	6.101038	1	6.101038	0.743745	0.4030	
C^2	0.993775	1	0.993775	0.121146	0.7330	
D^2	5.522035	1	5.522035	0.673162	0.4257	
Residual	114.8438	14	8.20313			
Lack of Fit	114.3733	10	11.43733	97.23971	0.0002	Significant
Pure Error	0.47048	4	0.11762			
Cor Total	483.4666	28				

it is observed that increased water jet pressure and decreased traverse rate lead to increased DOC and further observed that increases in abrasive flow rate and abrasive particle size result in higher DOC.

3.4 Analysis of Surface Roughness for Al 7075 + 10% SiC

Table 6 (S. No. 1–9) indicates that fine surface finish values are achieved by varying abrasive mesh size (#80 – #120) and abrasive flow rate (240–440 g/min. From the analysis (Table6, S. No. 1–54 and Fig. 5), it is observed that the combinations of input process parameter and their levels such as low abrasive mesh size, high abrasive flow rate, high water jet pressure and low traverse rate result in better surface finish (2.1 μm) for Al 7075 + 10% SiC. Due to the fact that smaller size of abrasive is likely to possess lesser kinetic energy than resulting in better Surface finish, higher size of abrasive is likely to possess higher kinetic energy than resulting in better surface

Table 5 Analysis of variance table for DoC (Al 7075 + SiC 10%)

Source	Sum of squares	d*f*	Mean square	*F* value	*p*-value Prob > *F*	
Model	368.6228	14	26.3302	3.209775	0.0184	Significant
A-abrasive mesh	120.7771	1	120.7771	14.72329	0.0018	
B-AFR	18.1548	1	18.1548	2.213155	0.1590	
C-water pressure	5.400208	1	5.400208	0.658311	0.4307	
D-reaverse rate	145.0465	1	145.0465	17.68185	0.0009	
AB	4.0401	1	4.0401	0.492507	0.4943	
AC	1.357225	1	1.357225	0.165452	0.6903	
AD	41.4736	1	41.4736	5.055826	0.0412	
BC	2.088025	1	2.088025	0.25454	0.6217	
BD	6.786025	1	6.786025	0.827248	0.3785	
CD	5.736025	1	5.736025	0.699248	0.4171	
A^2	1.812327	1	1.812327	0.220931	0.6456	
B^2	6.101038	1	6.101038	0.743745	0.4030	
C^2	0.993775	1	0.993775	0.121146	0.7330	
D^2	5.522035	1	5.522035	0.673162	0.4257	
Residual	114.8438	14	8.20313			
Lack of Fit	114.3733	10	11.43733	97.23971	0.0002	Significant
Pure Error	0.47048	4	0.11762			
Cor Total	483.4666	28				

finish. Similarly, it is observed that increased water jet pressure and decreased traverse rate lead to better surface finish, and further observed that increases in abrasive flow rate and abrasive particle size result in better Surface finish.

4 Conclusion

In this present work, an attempt is made to investigate the material removal rate, depth of cut and surface roughness of AWJM, for various input parameters. In this study, aluminum alloy (AL7075) is reinforced with 10% SiC by using stir casting process. The experiments are conducted using RSM with Box–Behnken design. The signification AWJM process parameters and their levels are identified for achieving

Table 6 Analysis of variance table for surface roughness

Source	Sum of squares	d*f*	Mean square	*F* value	*p*-value Prob > *F*	
Model	2.938214	14	0.209872	0.434522	0.9346	significant
A-abrasive mesh	1.198272	1	1.198272	2.480917	0.1376	
B-AFR	0.449694	1	0.449694	0.931052	0.3510	
C-water pressure	0.000533	1	0.000533	0.001104	0.9740	
D-reverse rate	0.052404	1	0.052404	0.108498	0.7467	
AB	0.026732	1	0.026732	0.055347	0.8174	
AC	0.107912	1	0.107912	0.223423	0.6437	
AD	0.044944	1	0.044944	0.093053	0.7648	
BC	0.273006	1	0.273006	0.565235	0.4646	
BD	0.14402	1	0.14402	0.298181	0.5936	
CD	0.118336	1	0.118336	0.245004	0.6283	
A^2	0.155436	1	0.155436	0.321816	0.5795	
B^2	0.000167	1	0.000167	0.000346	0.9854	
C^2	0.004624	1	0.004624	0.009574	0.9234	
D^2	0.364878	1	0.364878	0.755447	0.3994	
Residual	6.761939	14	0.482996			
Lack of Fit	2.893358	10	0.289336	0.299165	0.9446	Significant
Pure Error	3.868581	4	0.967145			
Cor Total	9.700153	28				

higher MRR, DoC and fine surface roughness. This investigation revealed the choice of #80 mesh size garnet for achieving the higher MRR of AWJM in Al7075 + SiC. MMCs can depend on the size of SiC particulate in MMCs. Hence, the combinations of input process parameter and their levels are recommended for higher MRR from the analysis of optimal value that are abrasive mesh size (#80), abrasive flow rate (440 g/min), water jet pressure (275 MPa) and traverse rate (60 mm/min), and the minimum MRR can be achieved by high abrasive mesh size (#120), abrasive flow rate (240 g/min), water jet pressure (125 MPa) and traverse rate (120 mm/min). Similarly, higher DoC is achieved with size (#80) and lower DoC is achieved with size (#120). Due to the fact that smaller size of abrasive is likely to possess lesser kinetic energy than resulting in lower DoC, higher size of abrasive is likely to possess higher kinetic energy than resulting in higher DoC. Similarly, it is observed that increased water jet pressure and decreased traverse rate lead to increase DoC, and further observed that increases in abrasive flow rate and abrasive particle size (μm) result in higher DoC. It is observed that better surface finish is achieved with size (#80), and rough surface finish is achieved with size (#120). Due to the fact that

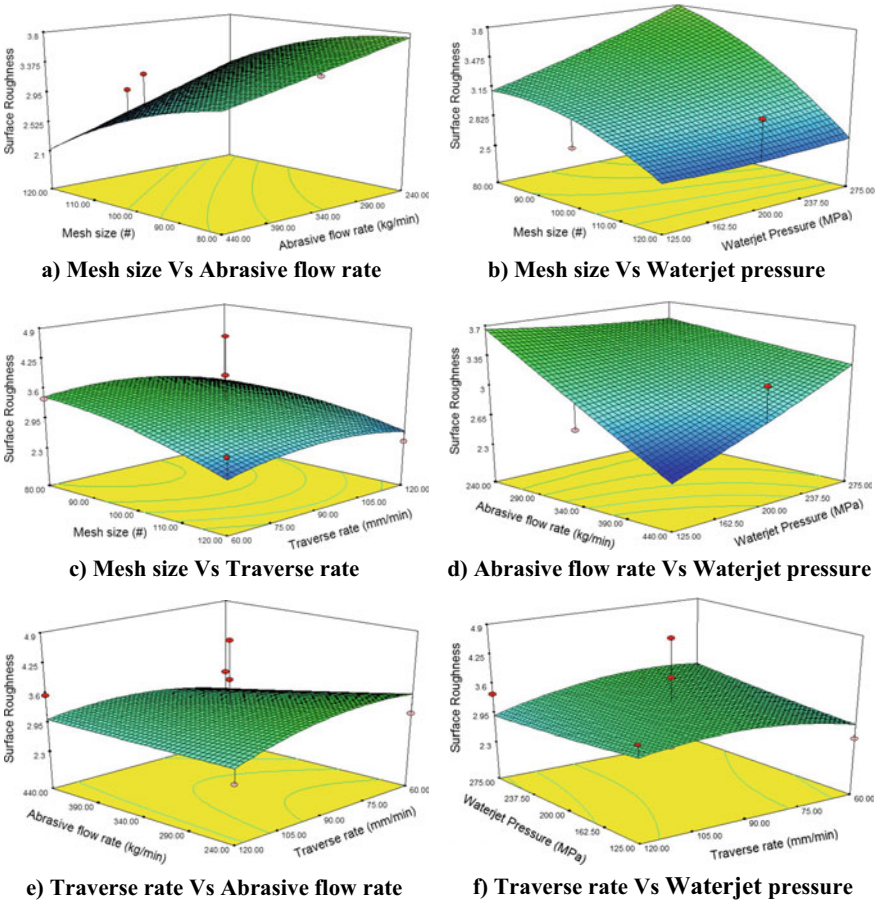

a) Mesh size Vs Abrasive flow rate

b) Mesh size Vs Waterjet pressure

c) Mesh size Vs Traverse rate

d) Abrasive flow rate Vs Waterjet pressure

e) Traverse rate Vs Abrasive flow rate

f) Traverse rate Vs Waterjet pressure

Fig. 5 Response surface of surface roughness (Al 7075 + 10% SiC) for various combinations

smaller size of abrasive is likely to possess lesser kinetic energy than resulting in better surface finish, higher size of abrasive is likely to possess higher kinetic energy than resulting in better surface finish. Similarly, it is observed that increased water jet pressure and decreased traverse rate lead to better surface finish, and further observed that increases in abrasive flow rate and abrasive particle size result in better surface finish.

References

1. Shukla R (2017) Experimentation investigation of abrasive water jet machining parameters using Taguchi and evolutionary optimization techniques. Swarm Evol Comput 32:167–183

2. Jurisevic B (2004) Monitoring of abrasive water jet (AWJ) cutting using sound detection. Int J Adv Manuf Technol 24:733–737
3. Savrun E (1988) Surface characterization of SiC whisker/2124 aluminum and Al_2O_3 composites machined by abrasive waterjet. J Mater Sci 23:1453–1458
4. Hamatani G (1990) Machinability of high temperature composites by abrasive waterjet. J Eng Mater Technol 318–386
5. Ramulu M, Raju SP (1993) Hydro-abrasive erosion characteristic of 30 vol%SiC/6061-T6 Al composite at shallow impact angles. Wear 166:55–63
6. Srinivas S, Rameshbabu N (2011) Role of garnet and silicon carbide in abrasive waterjet of aluminum-silicon carbide particulate metal matrix composites. Int J Appl Res Mech Eng 109–122
7. Muller F, Monaghan J (2000) Non-conventional machining of particle reinforced metal matrix composite. Int J Mach Tools Manuf 1351–1366
8. Momber AW, Kovacevic R (1998) Principle of abrasive waterjet machining. Springer, London
9. Kovacevic R, Hashish M, Mohan R, Ramulu M, Kim TJ, Geskin ES (1997) State of the art of research and development in abrasive waterjet machining . Trans ASME J Manuf Sci Eng 119:776–785
10. Hashish M (1989) A model for abrasive water jet (AWJ) machining. Trans ASME J Eng Mater Technol 3:154–162
11. Kovacevic R, Fang M (1994) Modeling of the influence of the abrasive waterjet cutting parameters on the depth of cut based on fuzzy rules. Int J Mach Tools Manuf 55–72
12. Fredin J, Jonsson A (2011) Experimentation on piercing with abrasive waterjet. World Acad Sci, Eng Technol 5:11–21
13. Brandt C, Louis H, Meier G, Tebbing G (1994) Abrasive suspension jets at working pressures up to 200MPs. Jet Cut Technol, Allen, pp 489–509
14. Kovacevic R (1991) A new sensing system to monitor Abrasive waterjet nozzle wear. J Mater Process Technol 28:117–125
15. Kovacevic R (1992) Monitoring the depth of the waterjet penetration. Int J Mach Tools Manuf 32:725–736